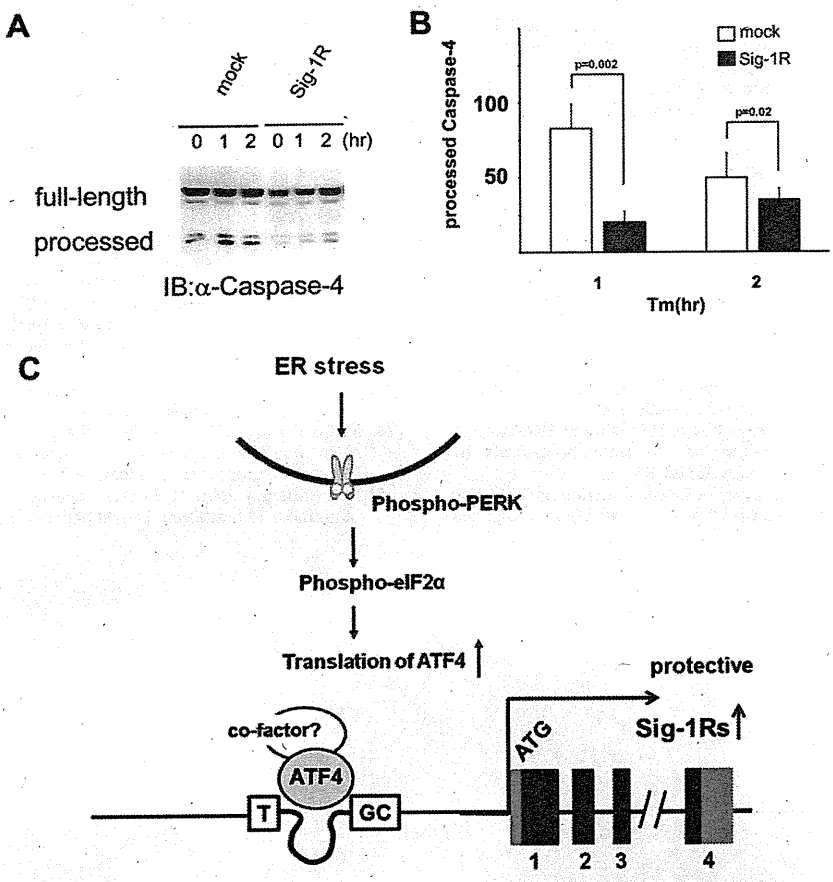

Fig. 4. (A) Sig-1Rs inhibits Caspase-4 processing. Processing of Caspase-4 in ER stress between Sigma-1Rs transfectant and mock transfectant were compared. Cells were treated with 1 μg/ml of Tm, for the indicated period. (B) Protein levels of processed Caspase-4 in Fig. 4A were quantified; values are means ± S.D. from three independent experiments. (C) Schematic representation of the results in this study. Sig-1Rs were upregulated via PERK/eIF2α/ATF4 pathway in ER stress and ameliolate cell death signaling. Pathogenesis with two polymorphism (T-485A, GC-241-240TT) might be caused by impediment of Sig-1Rs induction by ATF4.

pathogenic polymorphisms (T-485A or GC-241-240TT) in the 5′ upstream region, luciferase activity in ER stress by ATF4 were reduced. These data indicate that the nucleotide site -485T and -241-240GC were important for the binding with ATF4 (Fig. 4C).

In this study, we could not identify CARE-like element; known as ATF4 binding element, within the 5′ promoter region (−582 to −156). ATF4 is known to be bound with CARE-like element and induces target genes by interaction with C/EBP [25]. One possible explanation is ATF4 might compose complex with other unknown co-factors and induce Sig-1Rs expression.

Although additional studies are necessary to understand the detailed function of Sig-1Rs and mechanism regulating Sig-1Rs expression, our present study is the first report identifying the transcription factor ATF4 regulating Sig-1Rs expression to execute protective function. This pathway upregulating Sig-1Rs expression might become potential therapeutic target. And this result might provide the clue to prevent mental disorders from cell vulnerability.

Acknowledgments

We thank Drs T. Nakagawa (Gifu University School of Medicine) for ATF4-shRNA-pSUPER plasmid, D. Ron (New York University School of Medicine) for ATF4 plasmid, T. Hayashi (NIMH) for Sigma-1R plasmids and generous advice for this study. This work was supported by the Strategic Research Program for Brain Science of the Ministry of Education, Culture, Sports, Science and Technology of Japan.

Appendix A. Supplementary data

Supplementary data associated with this article can be found, in the online version, at doi:10.1016/j.bbrc.2011.10.113.

References

[1] M.J. Gething, J. Sambrook, Protein folding in the cell, Nature 355 (1992) 33–45.
[2] L. Ellgaard, M. Molinari, A. Helenius, Setting the standards: quality control in the secretory pathway, Science 286 (1999) 1882–1888.
[3] D. Ron, Translational control in the endoplasmic reticulum stress response, J. Clin. Invest. 110 (2002) 1383–1388.
[4] D.T. Rutkowski, R.J. Kaufman, A trip to the ER: coping with stress, Trends Cell Biol. 14 (2004) 20–28.
[5] M. Swift, R.G. Swift, Wolframin mutations and hospitalization for psychiatric illness, Mol. Psychiatry 10 (2005) 799–803.
[6] C. Kakiuchi, K. Iwamoto, M. Ishiwata, M. Bundo, T. Kasahara, I. Kusumi, T. Tsujita, Y. Okazaki, S. Nanko, H. Kunugi, T. Sasaki, T. Kato, Impaired feedback regulation of XBP1 as a genetic risk factor for bipolar disorder, Nat. Genet. 35 (2003) 171–175.
[7] M.F. Grunebaum, H.C. Galfalvy, Y.Y. Huang, T.B. Cooper, A.K. Burke, M. Agnello, M.A. Oquendo, J.J. Mann, Association of X-box binding protein 1 (XBP1) genotype with morning cortisol and 1-year clinical course after a major depressive episode, Int. J. Neuropsychopharmacol. 12 (2009) 281–283.
[8] T. Hayashi, T. Su, The sigma receptor: evolution of the concept in neuropsychopharmacology, Curr. Neuropharmacol. 3 (2005) 267–280.
[9] T. Hayashi, T.P. Su, Sigma-1 receptor chaperones at the ER-mitochondrion interface regulate Ca(2+) signaling and cell survival, Cell 131 (2007) 596–610.
[10] C. Katnik, W.R. Guerrero, K.R. Pennypacker, Y. Herrera, J. Cuevas, Sigma-1 receptor activation prevents intracellular calcium dysregulation in cortical neurons during in vitro ischemia, J. Pharmacol. Exp. Ther. 319 (2006) 1355–1365.

[11] A.D. Weissman, M.F. Casanova, J.E. Kleinman, E.D. London, E.B. De Souza, Selective loss of cerebral cortical sigma but not PCP binding sites in schizophrenia, Biol. Psychiatry 29 (1991) 41–54.
[12] R. Miyatake, A. Furukawa, S. Matsushita, S. Higuchi, H. Suwaki, Functional polymorphisms in the sigma1 receptor gene associated with alcoholism, Biol. Psychiatry 55 (2004) 85–90.
[13] H. Ishiguro, T. Ohtsuki, M. Toru, M. Itokawa, J. Aoki, H. Shibuya, A. Kurumaji, Y. Okubo, A. Iwawaki, K. Ota, H. Shimizu, H. Hamaguchi, T. Arinami, Association between polymorphisms in the type 1 sigma receptor gene and schizophrenia, Neurosci. Lett. 257 (1998) 45–48.
[14] T. Mitsuda, Y. Hayakawa, M. Itoh, K. Ohta, T. Nakagawa, ATF4 regulates gamma-secretase activity during amino acid imbalance, Biochem. Biophys. Res. Commun. 352 (2007) 722–727.
[15] P.D. Lu, H.P. Harding, D. Ron, Translation reinitiation at alternative open reading frames regulates gene expression in an integrated stress response, J. Cell Biol. 167 (2004) 27–33.
[16] M. Sakata, Y. Kimura, M. Naganawa, K. Oda, K. Ishii, K. Chihara, K. Ishiwata, Mapping of human cerebral sigma1 receptors using positron emission tomography and [11C] SA4503, Neuroimage 35 (2007) 1–8.
[17] M. Calfon, H. Zeng, F. Urano, J.H. Till, S.R. Hubbard, H.P. Harding, S.G. Clark, D. Ron, IRE1 couples endoplasmic reticulum load to secretory capacity by processing the XBP-1 mRNA, Nature 415 (2002) 92–96.
[18] S. Luo, P. Baumeister, S. Yang, S.F. Abcouwer, A.S. Lee, Induction of Grp78/BiP by translational block: activation of the Grp78 promoter by ATF4 through and upstream ATF/CRE site independent of the endoplasmic reticulum stress elements, J. Biol. Chem. 278 (2003) 37375–37385.
[19] A.H. Lee, N.N. Iwakoshi, L.H. Glimcher, XBP-1 regulates a subset of endoplasmic reticulum resident chaperone genes in the unfolded protein response, Mol. Cell Biol. 23 (2003) 7448–7459.
[20] K. Haze, H. Yoshida, H. Yanagi, T. Yura, K. Mori, Mammalian transcription factor ATF6 is synthesized as a transmembrane protein and activated by proteolysis in response to endoplasmic reticulum stress, Mol. Biol. Cell 10 (1999) 3787–3799.
[21] J. Hitomi, T. Katayama, Y. Eguchi, T. Kudo, M. Taniguchi, Y. Koyama, T. Manabe, S. Yamagishi, Y. Bando, K. Imaizumi, Y. Tsujimoto, M. Tohyama, Involvement of Caspase-4 in endoplasmic reticulum stress-induced apoptosis and Abeta-induced cell death, J. Cell Biol. 165 (2004) 347–356.
[22] D.H. Levin, R. Petryshyn, I.M. London, Characterization of double-stranded-RNA-activated kinase that phosphorylates alpha subunit of eukaryotic initiation factor 2 (eIF-2 alpha) in reticulocyte lysates, Proc. Natl. Acad. Sci. USA 77 (1980) 832–836.
[23] R.C. Wek, eIF-2 kinases: regulators of general and gene-specific translation initiation, Trends Biochem. Sci. 19 (1994) 491–496.
[24] M. Qu, F. Tang, L. Wang, H. Yan, Y. Han, J. Yan, W. Yue, D. Zhang, Associations of ATF4 gene polymorphisms with schizophrenia in male patients, Am. J. Med. Genet. B Neuropsychiatr. Genet. 147B (2008) 732–736.
[25] M.S. Kilberg, J. Shan, N. Su, ATF4-dependent transcription mediates signaling of amino acid limitation, Trends Endocrinol. Metab. 20 (2009) 436–443.

J Bone Miner Metab (2010) 28:131–138
DOI 10.1007/s00774-009-0117-z

ORIGINAL ARTICLE

Regulation of ER molecular chaperone prevents bone loss in a murine model for osteoporosis

Shin-ichiro Hino · Shinichi Kondo · Kazuya Yoshinaga · Atsushi Saito · Tomohiko Murakami · Soshi Kanemoto · Hiroshi Sekiya · Kazuyasu Chihara · Yuji Aikawa · Hideaki Hara · Takashi Kudo · Tomohisa Sekimoto · Taro Funamoto · Etsuo Chosa · Kazunori Imaizumi

Received: 8 April 2009 / Accepted: 1 July 2009 / Published online: 17 September 2009

Abstract Endoplasmic reticulum (ER) stress response is important for protein maturation in the ER. Some murine models for bone diseases have provided significant insight into the possibility that pathogenesis of osteoporosis is related to ER stress response of osteoblasts. We examined a possible correlation between osteoporosis and ER stress response. Bone specimens from 8 osteoporosis patients and 8 disease-controls were used for immunohistochemical analysis. We found that ER molecular chaperones, such as BiP (immunoglobulin heavy-chain binding protein) and PDI (protein-disulfide isomerase) are down-regulated in osteoblasts from osteoporosis patients. Based on this result, we hypothesized that up-regulation of ER molecular chaperones in osteoblasts could restore decreased bone formation in osteoporosis. Therefore, we investigated whether treatment of murine model for osteoporosis with BIX (BiP inducer X), selective inducer BiP, could prevent bone loss. We found that oral administration of BIX effectively improves decline in bone formation through the activation of folding and secretion of bone matrix proteins. Considering these results together, BIX may be a potential therapeutic agent for the prevention of bone loss in osteoporosis patients.

Keywords Osteoporosis · Osteoblast · BiP · BIX · Endoplasmic reticulum stress response

S. Hino · S. Kondo · K. Yoshinaga · A. Saito · T. Murakami · S. Kanemoto · H. Sekiya · K. Chihara · Y. Aikawa · K. Imaizumi (✉)
Division of Molecular and Cellular Biology, Department of Anatomy, Faculty of Medicine, University of Miyazaki, Kihara 5200, Kiyotake, Miyazaki 889-1692, Japan
e-mail: imaizumi@med.miyazaki-u.ac.jp

H. Hara
Department of Biofunctional Evaluation, Molecular Pharmacology, Gifu Pharmaceutical University, 5-6-1 Mitahora-higashi, Gifu 502-8585, Japan

T. Kudo
Department of Clinical Neuroscience, Psychiatry, Graduate School of Medicine, Osaka University, 2-2 Yamadaoka, Suita, Osaka 565-0871, Japan

T. Sekimoto · T. Funamoto · E. Chosa
Department of Orthopaedic Surgery, Faculty of Medicine, University of Miyazaki, Kihara 5200, Kiyotake, Miyazaki 889-1692, Japan

Introduction

When cells synthesize secretory proteins in amounts that exceed the capacity of the folding apparatus, unfolded proteins accumulate in the endoplasmic reticulum (ER). To alleviate such a stressful situation (ER stress), eukaryotic cells activate a series of self-defense mechanisms referred to collectively as the ER stress response or unfolded protein response (UPR) [1–3]. A malfunction of the UPR caused by aging, genetic mutations, or environmental factors can result in various diseases such as diabetes and neurodegenerative disorders [4, 5].

Osteoporosis is characterized by reduced bone mass, alterations in the microarchitecture of bone tissue, reduced bone strength, and an increased risk of fracture [6]. Many factors influence the risk of osteoporosis, including genetics, diet, physical activity, medication, and coexisting diseases, but the pathogenesis of osteoporosis still remains unclear. A very large number of genes have been identified as possible candidates for the regulation of bone mass and susceptibility to osteoporotic fractures [7]. Wolcott-Rallison syndrome

(WRS) is a rare autosomal recessive disorder that is characterized by permanent neonatal insulin-dependent diabetes, severe epiphyseal dysplasia, and osteoporosis [8]. The syndrome results from mutations in the gene encoding the eukaryotic translation initiation factor 2-kinase 3 (EIF2AK3, also called PERK or PEK), one of the major ER stress transducers [9]. EIF2AK3 deficient mice also exhibited skeletal defects included deficient mineralization, osteoporosis and abnormal compact bone development [10]. ATF4 is another ER stress-related gene and is a substrate for RSK2 (ribosomal serine/threonine kinase 2). ATF4-deficient mice showed a delay in ossification and osteopenia [11]. Patients with Coffin-Lowry syndrome, which is an X-linked disease characterized by mental retardation, delayed bone age, delayed closure of the fontanelle, and short stature, have mutations in RSK2. Both ATF4−/− mice and RSK2−/− mice showed disturbance in type I collagen production [11]. Furthermore, abnormal ER retention of type I procollagen was observed in PERK−/− osteoblasts [12]. Taken together, normal ER stress responses could play important roles in type I collagen synthesis and secretion.

The phenotypes of these murine models and human bone disease suggest that pathogenesis of bone disease, such as osteopenia and osteoporosis, is related to ER stress response of osteoblasts. However, little has been reported on the relationship between osteoporosis and ER stress response. In this report, we analyzed whether development of osteoporosis correlates with ER stress response in osteoblasts of osteoporosis patients.

BiP (immunoglobulin heavy-chain binding protein) is one of the ER molecular chaperones, and is induced in response to ER stress. BiP serves to restore folding of misfolded or incompletely assembled proteins [13, 14] and expression of BiP protects against various types of cell death induced by ER stress [15, 16]. A chemical compound, BIX (BiP inducer X), 1-(3,4-dihydroxyphenyl)-2-thiocyanato-ethanone (Fig. 3a), was developed as an inducer of *BiP* mRNA [17]. In this paper, we also investigated whether treatment of murine model for osteoporosis with BIX could effectively prevent bone loss.

Materials and methods

Patient details

Clinical osteoporosis was determined from the bone mineral density (BMD) by radiographic absorptiometry or dual energy X-ray absorptiometry (DXA). Bone samples used in this study were from 8 osteoporosis patients aged 53–88 years (Table 1, patient I–P). As control samples, 8 bone specimens from disease–controls were collected aged 35–77 years, undergoing surgical procedures such as amputation for hip osteoarthritis (Table 1, patient A–H).

Histological processing

Bone specimens were fixed at the earliest possible opportunity in 10% neutral formalin and then decalcified with 10% EDTA. Hematoxylin–Eosin (HE) was performed using 6 μm paraffin sections and standard protocols.

For immunohistochemistry, dewaxed paraffin sections were pretreated with 3% hydrogen peroxide in PBS for 5 min and treated with 1% bovine serum albumin in PBS for 60 min. Sections were subsequently incubated with mouse anti-KDEL antibody (MBL) or mouse anti-PDI antibody (Affinity BioReagents) followed by an incubation with horseradish peroxidase (HRP)-conjugated anti-mouse IgG antibody (GE Healthcare). The immunoreaction was visualized with DAB stain (Sigma). For immunofluorescence, primary antibodies were visualized with alexa-conjugated goat anti-mouse IgG (Molecular Probes). Stained sections were viewed using a confocal microscope (FV1000D, OLYMPUS).

Quantification of immunofluorescence

To quantify the expression levels of BiP and PDI, fluorescence images of stained sections were measured by Lumina Vision software (Mitani Corporation). Obtained fluorescence intensity was normalized to the total surface area of osteoblasts.

Cell culture materials

Primary cultures of osteoblasts were prepared from the calvaria of postnatal 4 days in C57BL/6 mice and were grown in alpha modified Eagle's medium supplemented with 10% fetal calf serum. To confirm that the osteoblastic genes were expressed in primary culture, the mRNAs for *Alkaline phosphatase* (*Alp*) and *osteocalcin* were examined using RT-PCR at 14 days after the plating of cells. The amount of secreted osteopontin in the supernatants from primary osteoblasts was determined by ELISA using commercial kits (R&D Systems). The primers used for amplification were as follows: Alp, 5′-GCCCTCTCCAAGACATATA-3′ and 5′-CCATGATCACGTCGATATCC-3′; osteocalcin, 5′-AA GCAGGAGGGCAATAAGGT-3′ and 5′-AGCTGCTGTG ACATCCATAC-3′.

RNA extraction and real-time RT-PCR

Female ICR mice (7-week old) were orally administered BIX at 10 or 30 mg/kg or vehicle for 24 h, then the tibia from the hind limb was collected. Total RNA was isolated

Table 1 Information on osteoporosis patients and controls

Patient	Disease	Osteoporosis (+/−)	Site of biopsy	Sex (M/F)	Age (years)	'Active' osteoblast	Remarks
A	Knee osteoarthritis	−	Condyle of femur	F	77	++	Figs. 1, 2
B	Hip osteoarthritis	−	Femur head	F	68	++	
C	Hip osteoarthritis	−	Femur head	M	58	++	
D	Hip osteoarthritis	−	Femur head	M	60	++	
E	Hip osteoarthritis	−	Femur head	F	78	+	
F	Hernia of intervertebral disk (L5/S1)	−	Spine (L5)	M	35	+	
G	Hernia of intervertebral disk (L4/L5)	−	Spine (L5)	M	72	+	
H	Hernia of intervertebral disk (L4/L5)	−	Vertebral arch (L4)	M	52	++	
I	Osteoporosis (mild)	+	Tibia	M	78	−	
J	Osteoporosis (mild)	+	Femur head	F	85	+	
K	Osteoporosis	+	Condyle of femur	F	88	−	
L	Osteoporosis	+	Spine (L4)	M	71	−	
M	Osteoporosis/rheumatoid arthritis	+	Condyle of femur	F	66	+	
N	Osteoporosis/rheumatoid arthritis	+	Condyle of femur	F	53	−	
O	Osteoporosis/knee osteoarthritis	+	Femur neck	F	81	−	
P	Osteoporosis	+	Spine (L2)	F	69	+	

++, Large population of active osteoblasts; +, small population of active osteoblasts; −, no active osteoblast (bone lining cell only)

from the tibia using an RNeasy Mini kit (Qiagen) and reverse transcribed using the High-Capacity cDNA Archive kit (Applied Biosystems). TaqMan real-time PCR was performed using specific primer sets of BiP and β-actin. The primers used for amplification were as follows: BiP, 5′-GT TTGCTGAGGAAGACAAAAAGCTC-3′ and 5′-CACTT CCATAGAGTTTGCTGATAATTG-3′; β-actin, 5′-TCCT CCCTGGAGAAGAGCTAC-3′ and 5′-TCCTGCTTGCT GATCCACAT-3′ Expression of mRNA for BiP and β-actin endogenous control was measured in each specimen with real-time PCR on an ABI PRISMs 7900HT Sequence Detection System (Applied Biosystems).

Ovariectomized mice

As a model for osteoporosis (estrogen deficiency), female ICR mice (20 to 36-week old) were either ovariectomized (OVX) or sham operated. After surgery, the mice were orally administered 10 or 30 mg/kg/day BIX for 8 weeks. The vehicle control group received 0.5% sodium calboxymethylcellulose solution. As a positive control, OVX mice were administered 17β-estradiol. Body weight and bone length were measured. The whole tibial bone mineral densities (BMD) were measured using a DCS-600EX (Aloka).

Statistics

Data are presented as the mean ± SE. The statistical significance of differences was evaluated using the Student's *t* test or Aspin-Welch's *t* test.

Ethics

Full consent was obtained prior to surgery and these studies were approved by the Miyazaki University Ethics Committees (date of issue: 5 February 2007, registration number: 323).

Results

Morphological analysis of osteoblasts from osteoporosis patients

Clinical osteoporosis was determined from the bone mineral density (BMD) by radiographic absorptiometry or dual energy X-ray absorptiometry (DXA) (Table 1, patient I–P). As control samples, 8 bone specimens from disease-controls were collected (Table 1, patient A–H). Compared with a previous report using human bone [18], there was no significant difference in the morphology between normal-control and 8 disease-control specimens. The reduction of bone mass with loss of trabecular bone and enlargement of medullary space were observed in all osteoporosis samples, as previously reported [19] (Fig. 1a, b). Moreover, consistent with a previous study [20], the bone marrow cavity was filled with adipocytes instead of stromal cells and hematopoietic cells. Although we could not detect any differences in the number of osteoblasts between osteoporosis and disease-control specimens, there was a morphological difference. Disease-control bone specimens showed a considerable

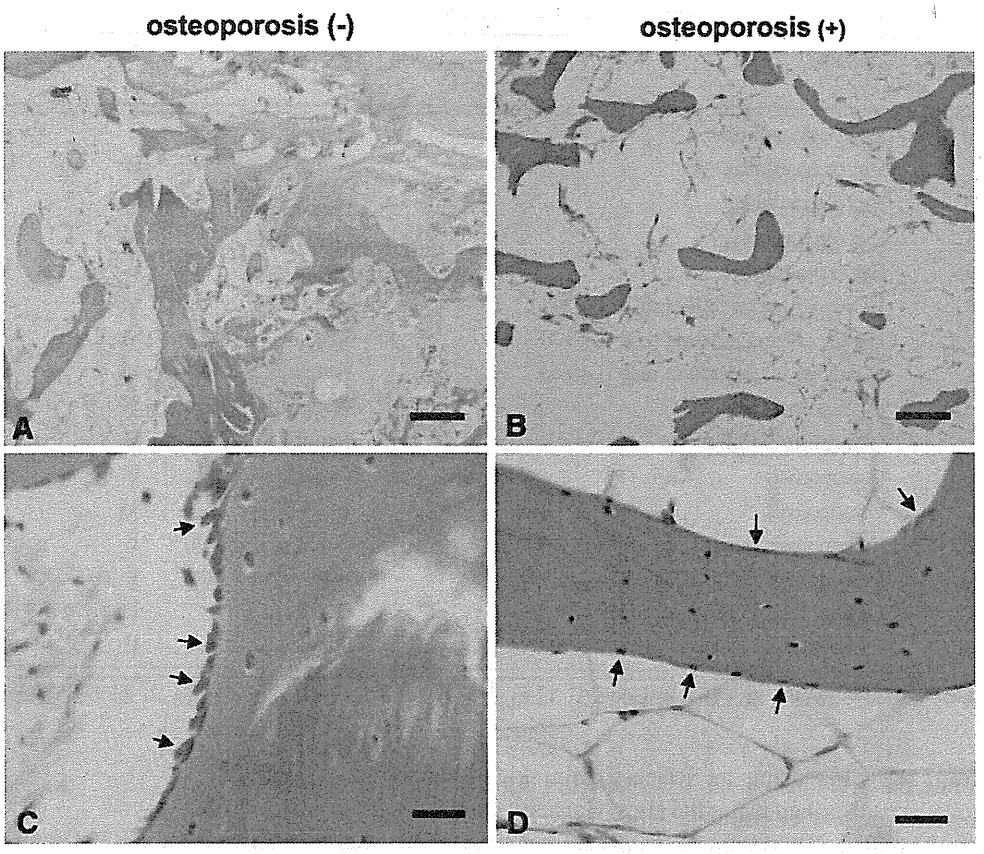

Fig. 1 Most osteoporosis osteoblasts are bone lining cells with decreased matrix synthesis. H&E staining of the condyle of the femur seen in controls (patient A; **a**) and osteoporosis patients (patient N; **b**). **c** Higher magnification of **a**. Osteoblasts with a cuboidal shape (*arrows*). **d** Higher magnification of **b**. Note, most osteoporosis osteoblasts are bone lining cells (*arrows*). *Scale bars* 500 μm (**a**, **b**), 50 μm (**c**, **d**)

population of 'active' osteoblasts with a cuboidal shape (Fig. 1c). On the other hand, notable flattened epithelium-like cells, called bone lining cells, were observed on the bone surface from osteoporosis patients (Fig. 1d). As shown in Table 1, osteoblasts from almost all patients that we examined showed this type of morphology.

Expression levels of ER stress-related genes are weaker in osteoporosis osteoblasts

To investigate whether ER stress occurs in human osteoblasts from osteoporosis patients, we next examined the expression level of the ER stress-related proteins BiP and PDI in osteoporosis and disease-control osteoblasts. Both BiP and PDI are up-regulated when ER stress occurs [21]. Immunohistochemical analysis using the anti-KDEL antibody which recognizes BiP protein, showed strong expression of the protein in disease-control osteoblasts (Fig. 2a, c). Immunoreactivity for BiP was weak in other cell types, such as osteocytes and blood cells. These staining patterns in disease-control osteoblasts showed that the level of BiP in the ER is high, indicating that there might be ER stress response that occurs physiologically in osteoblasts with a cuboidal shape. On the other hand, in osteoporosis osteoblasts, immunohistochemical analysis using the anti-KDEL antibody showed weak expression of the BiP protein in the cytosol around the nucleus (Fig. 2b, d). Strong immunoreactivity for PDI, which is also an ER stress-related protein, was observed in the ER of disease-control osteoblasts (Fig. 2e, g), but no immunoreactivity for PDI was observed in osteoblasts from osteoporosis patients (Fig. 2f, h). By quantitative analysis, as described in "Materials and methods", the expression levels of BiP and PDI were significantly decreased in osteoblasts from 8 osteoporosis patients compared with those from 8 disease-control specimens (Fig. 2i, j). These results indicate that ER stress response, including induction of ER molecular chaperones, is physiologically activated in cuboidal shaped active osteoblasts in the disease-controls. In contrast, it is down-regulated in bone lining cells from osteoporosis patients.

Based on these results, we hypothesized that induction of ER molecular chaperones could restore the decreased bone formation in osteoblasts from osteoporosis patients. Therefore, we next tested our hypothesis using a murine model for osteoporosis.

BIX induces BiP mRNA expression in mouse bone tissue

We used a chemical compound BIX (Fig. 3a), which has potential to induce BiP at the transcriptional level, for

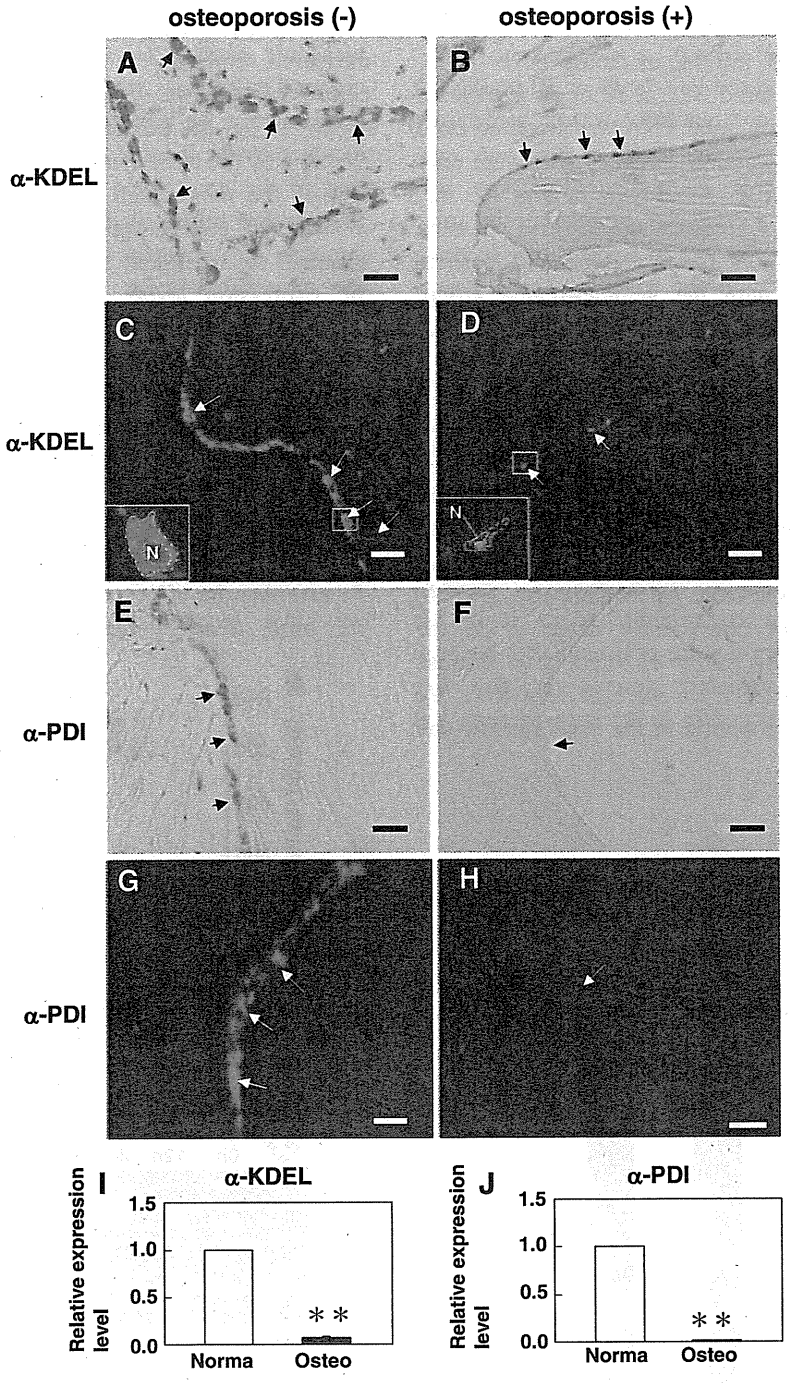

Fig. 2 Bone lining cells show weaker expression of ER stress-related genes. Immunohistochemistry for anti-KDEL that recognizes BiP, in the condyle of the femur seen in a control (patient A; **a**) and an osteoporosis patient (patient N; **b**). Immunofluorescence for anti-KDEL that recognizes BiP, in the spine seen in a control (patient G; **c**) and an osteoporosis patient (patient L; **d**). The *inset* is a higher magnification image of the *white box*. Cytosol and nucleus are encircled by dashed lines. *N* nucleus. Note, the immunoreactivity for KDEL (*arrows*) is weak in bone lining cells of the osteoporosis patient compared to the osteoblasts in the control. Immunohistochemistry for PDI protein in the condyle of the femur seen in a control (patient A; **e**) and an osteoporosis patient (patient N; **f**). Immunofluorescence for PDI protein, in the spine seen in a control (patient G; **g**) and an osteoporosis patient (patient L; **h**). Note, immunoreactivity for PDI (*arrows*) is notably weak in bone lining cells of the osteoporosis patient compared to control osteoblasts. **i** Quantitative analysis of BiP protein levels between (**c**) and (**d**). **j** Quantitative analysis of PDI protein levels between (**g**) and (**h**). These results shown (**i**, **j**) were normalized to the total surface area of osteoblasts. Note, there was no notable difference in the number of osteoblasts between osteoporosis patients and controls. The corresponding quantification results for BiP and PDI protein levels were expressed as the fold decrease compared with those in the control. Data are means ± SE, $n = 8$ (8 controls: patient A–H, 8 osteoporosis: patient I–P). $^{**}p < 0.01$ relative to the control. *Scale bars* 50 μm (**a**–**h**)

activation of declined osteoblasts. We first examined whether BIX induces *BiP* mRNA in mouse bone tissue. Mice were orally administered BIX at 10 or 30 mg/kg. At 24 h after the administration, total RNA was prepared from the tibia and then the expression levels of BiP were analyzed by real-time RT-PCR. As shown in Fig. 3b, *BiP* mRNA in tibia showed a tendency to increase in mice treated with BIX at 10 mg/kg and to significantly increase at 30 mg/kg, compared with the vehicle-treated group. These results indicate that oral administration of BIX induces *BiP* mRNA in mouse bone tissues.

BIX promotes secretion of osteopontin

To investigate the effects of BIX on bone matrix formation of osteoblasts, we measured the amounts of secreted bone matrix protein from the primary osteoblasts. Initially, we tried to measure the secreted osteocalcin by ELISA. However, we could not consistently detect it in the supernatants of the primary culture of osteoblasts, because the levels of secreted osteocalcin were at very low. We then tried to measure osteopontin in the supernatants, and we could easily and reproducibly detect it. Therefore, we measured secreted osteopontin after treatment of primary cultured osteoblasts with 5 μM BIX for 12, 16, or 24 h. As shown in Fig. 4a, secretion of osteopontin was significantly elevated by the treatment with BIX for 24 h compared with that of the non-treated control. We confirmed that BIX induced *BiP* mRNA in the primary osteoblasts (Fig. 4b). In contrast, the treatment of BIX did not have an impact on the expression levels of *ALP* and *osteocalcin* mRNA (Fig. 4b), indicating that BIX could not affect the differentiation or maturation of osteoblasts. These results indicate that treatment with BIX enhances bone matrix secretion leading to augmentation of bone formation through facilitating protein folding in the ER of osteoblasts.

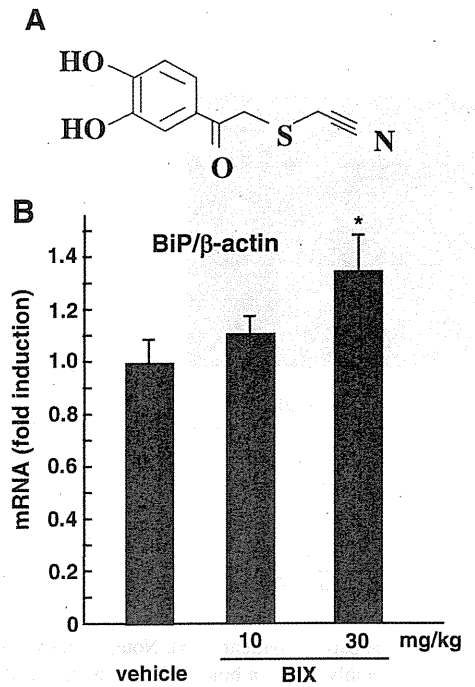

Fig. 3 BIX induces *BiP* mRNA in the tibia of mice. **a** Chemical structure of BIX (BiP inducer X), 1-(3,4-dihydroxy-phenyl)-2-thiocyanato-ethanone. **b** Real-time RT–PCR analysis of *BiP* mRNA in tibial bone. Mice were orally administered BIX (10 or 30 mg/kg) or vehicle for 24 h. Total RNA prepared from the tibia was subjected to real-time RT-PCR using specific primer sets of BiP and *β*-actin. The results shown were normalized by the *β-actin* mRNA levels, and the corresponding quantification results for the *BiP* mRNA levels were expressed as the fold induction compared with that of the vehicle control group. Data are means ± SE, $n = 5$. $^*p < 0.05$ vs. vehicle (Student's *t* test)

BIX prevents bone loss in ovariectomized mice

To examine the effects of BIX on bone formation in vivo, we used ovariectomized (OVX) osteoporosis mouse

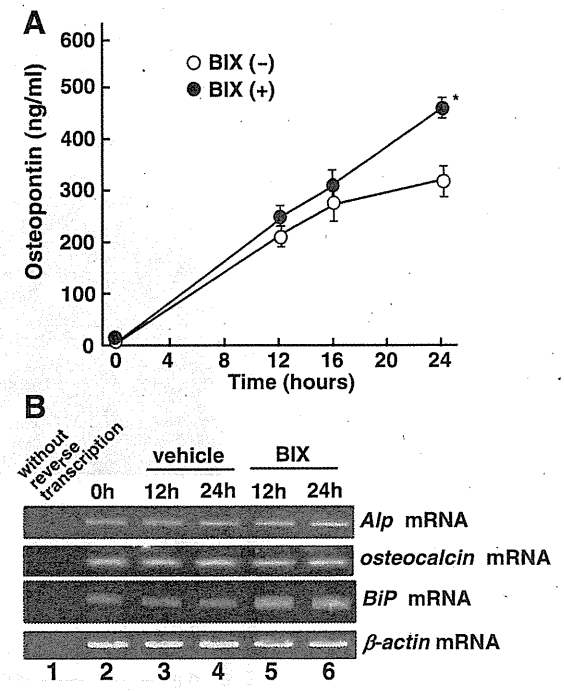

Fig. 4 BIX promotes secretion of osteopontin. **a** Primary cultured osteoblasts were treated with 5 μM BIX or without for 12, 16, or 24 h. Supernatants were analyzed for secretion of osteopontin by ELISA. Data are means ± SE from five independent experiments. $^*p < 0.05$ vs. vehicle (Student's *t* test). **b** Total RNA prepared from the primary cultured osteoblasts was subjected to RT-PCR using specific primer sets of Alkaline phosphatase (Alp), osteocalcin, BiP, and *β*-actin. RT-PCR analysis of primary cultured osteoblasts at 14 days after the plating (*lane 2*). PCR reaction was subjected without reverse transcription as a control (*lane 1*). The expression levels of *Alp* and *osteocalcin* mRNAs were high, indicating that cultured cells prepared from the calvaria are sufficiently differentiated to mature osteoblasts. The effects of BIX on the Alp, osteocalcin, and BiP expression (*lane 3–6*). Primary cultured osteoblasts were treated with vehicle (*lane 3 and 4*) or 5 μM BIX (*lane 5 and 6*) for 12 or 24 h

models. OVX mice were orally administered BIX at 10 or 30 mg/kg for 8 weeks. The ovariectomy did not affect body weight change and bone length in each group (data not shown). The whole tibial bone mineral density (BMD) was significantly decreased in OVX mice compared with the sham-operated group (Fig. 5). Consistent with previous studies [22, 23], the BMD loss in OVX mice was recovered by treatment with 17β-estradiol, but this treatment caused hyperplasia of the bone matrix. The administration of BIX into sham-operated mice did not affect their bone formation (data not shown). The administration of BIX into OVX mice significantly prevented the whole tibial BMD loss (at 10 and 30 mg/kg BIX) (Fig. 5). However, treatment with 30 mg/kg BIX showed weak effects on the improvement of bone loss compared with 10 mg/kg BIX. Treatment with 30 mg/kg BIX caused a decrease of voluntary exercise, indicating that treatment with high doses of BIX could cause some toxic effects in mice. It is possible that this toxicity weakens the effects of BIX on the facilitation of bone formation. In addition, pathologically abnormal findings were not observed in bone tissues of BIX-treated mice, different from the case of treatment with 17β-estradiol. The administration of BIX did not lead to alteration of TRAP positive osteoclasts numbers (data not shown), suggesting that BIX does not affect the activities of osteoclasts. These results indicate that oral administration of BIX effectively improves decline in bone formation of osteoporosis mouse models through acting on osteoblasts.

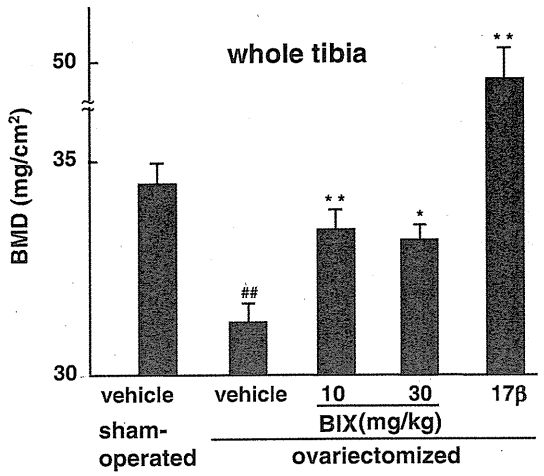

Fig. 5 BIX prevents bone loss in ovariectomized mice. Whole tibial BMD. Ovariectomized mice were orally administered 10 or 30 mg/kg/day BIX, or treated with 0.03 μg/mouse/day 17β-estradiol (17β) subcutaneously for 8 weeks after the operation. Data are means ± SE, $n = 11$ to 12. $^{\#\#}p < 0.01$ vs. sham vehicle (Student's t test). $^{*}p < 0.05$, $^{**}p < 0.01$ vs. OVX vehicle (Student's t test, Aspin-Welch's t test)

Discussion

In the present study, we have shown that control osteoblasts with a cuboidal shape strikingly express ER stress-related genes such as BiP and PDI (Fig. 2a, c), suggesting that an ER stress response occurs in 'active' osteoblasts. High-level secretory protein synthesis and secretion could lead to an overload of the ER in active osteoblasts and this could cause ER stress. It is conceivable that activation of the ER stress response is a physiological adaptation for osteoblasts to properly fold and secrete massive amounts of proteins as a protection against ER overload, and that this response is essential for osteoblasts to synthesize bone matrix.

In osteoporosis patients, most osteoblasts are bone lining cells and there are few active osteoblasts (Fig. 1d), suggesting that the loss of active osteoblasts is associated with the pathogenesis of osteoporosis and causes a reduction in matrix synthesis. Further, bone lining cells showed a weaker expression of ER stress-related genes such as BiP and PDI (Fig. 2b, d) and down-regulated ER stress response. The results are consistent with a declining bone matrix synthesis in osteoporosis bone lining cells. Taken together, folding capacity of secreted proteins in the ER could be declined in osteoblasts from the patients followed by augmentation of reduced bone formation.

It is well known that loss of estrogen is an important risk factor for pathogenesis of osteoporosis. Ovariectomy in the mice results in an increase in bone turnover rate and significant loss of trabecular bone, vertebral bodies and the metaphysis of long bones [24]. In this study, we also observed ovariectomy caused decrease in whole tibial BMD involving trabecular bone loss as shown in previous studies. Oral administration of BIX prevented whole tibial BMD loss of this mouse model. BIX is an inducer of ER molecular chaperone BiP. BiP has a potential to facilitate folding of proteins in the ER. The possible mechanisms responsible for prevention of bone loss and acceleration of bone formation by BIX are that induced BiP could increase folding capacity in the ER followed by facilitating secretion of bone matrix proteins from osteoblasts. This hypersecretion of bone matrix proteins by BIX could lead to an increase in the bone formation rate that superpasses bone resorption by osteoclasts. Although various agents have been developed for the treatment of osteoporosis, the majority of these reduce bone resorption by affecting osteoclast activity. Considering our finding that BIX accelerates the osteoblast-mediated bone formation, BIX could be an alternative therapeutic agent for high-turnover osteoporosis.

Acknowledgments We would like to thank Keisuke Goto for performing the surgeries and kindly making tissue available from

patients, as well as Ai Ikeda and Tomoko Kawanami for their technical assistance in the laboratory. This study was supported by the Program for Promotion of Fundamental Studies in Health Sciences of the National Institute of Biomedical Innovation, the Takeda Science Foundation, and the Mochida Memorial Foundation for Medical and Pharmaceutical Research.

References

1. Harding HP, Calfon M, Urano F, Novoa I, Ron D (2002) Transcriptional and translational control in the mammalian unfolded protein response. Annu Rev Cell Dev Biol 18:575–599
2. Patil C, Walter P (2001) Intracellular signaling from the endoplasmic reticulum to the nucleus: the unfolded protein response in yeast and mammals. Curr Opin Cell Biol 13:349–355
3. Schröder M, Kaufman RJ (2005) ER stress and the unfolded protein response. Mutat Res 569:29–63
4. Harding HP, Zeng H, Zhang Y, Jungries R, Chung P, Plesken H, Sabatini DD, Ron D (2001) Diabetes mellitus and exocrine pancreatic dysfunction in perk−/− mice reveals a role for translational control in secretory cell survival. Mol Cell 7:1153–1163
5. Zhao L, Longo-Guess C, Harris BS, Lee JW, Ackerman SL (2005) Protein accumulation and neurodegeneration in the woozy mutant mouse is caused by disruption of SIL1, a cochaperone of BiP. Nat Genet 37:974–979
6. Kanis JA, Melton LJIII, Christiansen C, Johnston CC, Khaltaev N (1994) The diagnosis of osteoporosis. J Bone Miner Res 9:1137–1141
7. Ralston SH, de Crombrugghe B (2006) Genetic regulation of bone mass and susceptibility to osteoporosis. Genes Dev 20:2492–2506
8. Wolcott CD, Rallison ML (1972) Infancy-onset diabetes mellitus and multiple epiphyseal dysplasia. J Pediatr 80:292–297
9. Delépine M, Nicolino M, Barrett T, Golamaully M, Lathrop GM, Julier C (2000) EIF2AK3, encoding translation initiation factor 2-alpha kinase 3, is mutated in patients with Wolcott–Rallison syndrome. Nat Genet 25:406–409
10. Zhang P, McGrath B, Li S, Frank A, Zambito F, Reinert J, Gannon M, Ma K, McNaughton K, Cavener DR (2002) The PERK eukaryotic initiation factor 2 alpha kinase is required for the development of the skeletal system, postnatal growth, and the function and viability of the pancreas. Mol Cell Biol 22:3864–3874
11. Yang X, Matsuda K, Bialek P, Jacquot S, Masuoka HC, Schinke T, Li L, Brancorsini S, Sassone-Corsi P, Townes TM, Hanauer A, Karsenty G (2004) ATF4 is a substrate of RSK2 and an essential regulator of osteoblast biology; implication for Coffin-Lowry Syndrome. Cell 117:387–398
12. Wei J, Sheng X, Feng D, McGrath B, Cavener DR (2008) PERK is essential for neonatal skeletal development to regulate osteoblast proliferation and differentiation. J Cell Physiol 217:693–707
13. Yoshida H (2007) ER stress and diseases. FEBS J 274:630–658
14. Ni M, Lee AS (2007) ER chaperones in mammalian development and human diseases. FEBS Lett 581:3641–3651
15. Katayama T, Imaizumi K, Sato N, Miyoshi K, Kudo T, Hitomi J, Morihara T, Yoneda T, Gomi F, Mori Y, Nakano Y, Takeda J, Tsuda T, Itoyama Y, Murayama O, Takashima A, George-Hyslop PS, Takeda M, Tohyama M (1999) Presenilin-1 mutations downregulate the signalling pathway of the unfolded-protein response. Nat Cell Biol 1:479–485
16. Rao RV, Peel A, Logvinova A, del Rio G, Hermel E, Yokota T, Goldsmith PC, Ellerby LM, Ellerby HM, Bredesen DE (2002) Coupling endoplasmic reticulum stress to the cell death program: role of the ER chaperone GRP78. FEBS Lett 514:122–128
17. Kudo T, Kanemoto S, Hara H, Morimoto N, Morihara T, Kimura R, Tabira T, Imaizumi K, Takeda M (2008) A molecular chaperone inducer protects neurons from ER stress. Cell Death Differ 15:364–375
18. Nampei A, Hashimoto J, Hayashida K, Tsuboi H, Shi K, Tsuji I, Miyashita H, Yamada T, Matsukawa N, Matsumoto M, Morimoto S, Ogihara T, Ochi T, Yoshikawa H (2004) Matrix extracellular phosphoglycoprotein (MEPE) is highly expressed in osteocytes in human bone. J Bone Miner Metab 22:176–184
19. Jowsey J, Phil D, Kelly PJ, Riggs BL, Bianco AJ Jr, Scholz DA, Gershon-Cohen J (1965) Quantitative microradiographic studies of normal and osteoporotic bone. J Bone Joint Surg Am 47:785–806
20. Justesen J, Stenderup K, Ebbesen EN, Mosekilde L, Steiniche T, Kassem M (2001) Adipocyte tissue volume in bone marrow is increased with aging and in patients with osteoporosis. Biogerontology 2:165–171
21. Kondo S, Murakami T, Tatsumi K, Ogata M, Kanemoto S, Otori K, Iseki K, Wanaka A, Imaizumi K (2005) OASIS, a CREB/ATF-family member, modulates UPR signalling in astrocytes. Nat Cell Biol 7:186–194
22. Takano-Yamamoto T, Rodan GA (1990) Direct effects of 17β-estradiol on trabecular bone in ovariectomized rats. Proc Natl Acad Sci USA 87:2127–2176
23. Kawaguchi H, Pilbeam CC, Vargas SJ, Morse EE, Lorenzo JA, Raisz LG (1995) Ovariectomy enhances and estrogen replacement inhibits the activity of bone marrow factors that stimulate prostaglandin production in cultured mouse calvariae. J Clin Invest 96:539–548
24. Omi N, Ezawa I (1995) The effect of ovariectomy on bone metabolism in rats. Bone 17:163S–168S

Pharmacology & Pharmacy, 2011, 2, 10-16
doi:10.4236/pp.2011.21002 Published Online January 2011 (http://www.SciRP.org/journal/pp)

Scientific Research

Restraint-Induced Expression of Endoplasmic Reticulum Stress-Related Genes in the Mouse Brain

Mitsue Ishisaka[1], Takashi Kudo[2], Masamitsu Shimazawa[1], Kenichi Kakefuda[1], Atsushi Oyagi[1], Kana Hyakkoku[1], Kazuhiro Tsuruma[1], Hideaki Hara[1]

[1]Molecular Pharmacology, Department of Biofunctional Evaluation, Gifu Pharmaceutical University; [2]Department of Psychiatry, Osaka University Graduate School of Medicine.
Email: hidehara@gifu-pu.ac.jp

Received October 26th, 2010; revised November 23rd, 2010; accepted November 30th, 2010.

ABSTRACT

Depression is a significant public health concern but its pathology remains unclear. Previously, increases in an endoplasmic reticulum (ER) stress-related protein were reported in the temporal cortex of subjects with major depressive disorder who had died by suicide. This finding suggests an association between depression and ER stress. The present study was designed to investigate whether acute stress could affect the ER stress response. Mice were immobilized for a period of 6 hr and then expression of ER stress response-related genes was measured by real-time PCR. We also used enzyme-linked immunosorbent assay for concomitant measurement of the plasma corticosterone levels in the mice. The effect of corticosterone on ER stress proteins was further investigated by treating mice with corticosterone for 2 weeks and then measuring ER protein expression by Western blotting. After a 6 hr restraint stress, mRNA levels of ER stress-related genes, such as the 78-kilodalton glucose regulated protein (GRP78), the 94-kilodalton glucose regulated protein (GRP94), and calreticulin, were increased in the cortex, hippocampus, and striatum of mouse brain. Blood plasma corticosterone level was also increased. In the corticosterone-treated mouse model, the expression of GRP78 and GRP94 was significantly increased in the hippocampus. These results suggest that acute stress may affect ER function and that ER stress may be involved in the pathogenesis of restraint stress, including the development of depression.

Keywords: *Corticosterone, Depression, Endoplasmic Reticulum Stress, Restraint Stress*

1. Introduction

Major depression, along with bipolar disorder, has become a common psychiatric disorder in modern society. About 1% of the population is estimated to be affected by major depression one or more times during their lifetime [1]. Even though extensive studies have led to a variety of hypotheses regarding the molecular mechanism underlying depression, the pathogenesis of this disorder remains to be fully elucidated.

The endoplasmic reticulum (ER) is the cell organelle where secretory and membrane proteins are synthesized and folded. It also functions as a Ca^{2+} store and resource of calcium signals. The disturbance of ER functions through events such as disruption of Ca^{2+} homeostasis, inhibition of protein glycosylation or disulfide bond formation, hypoxia and viral or bacterial infection, can result in the accumulation of unfolded or misfolded proteins and may trigger stress responses in the cell (ER stress). To overcome ER stress, an unfolded protein response (UPR) is invoked by the activation of several signaling pathways; this UPR promotes an adaptive response to ER stress and reestablishes homeostasis in the ER [2,3]. Molecular chaperones such as the 78-kilodalton glucose regulated protein (GRP78) and the 94-kilodalton glucose regulated protein are induced and promote correct protein folding. If the damage is too severe to repair, C/EBP-homologous protein (CHOP) and other factors are activated and induce cell apoptosis [4]. On the other hand, if misfolded protein aggregates into insoluble higher-order structures, it can give rise to various diseases. For example, rhodopsin misfolding causes autosomal dominant retinitis pigmentosa [5], while the accumulation of amyloid β-peptide is associated with Alzheimer's disease [6].

Some reports have also suggested a relationship between mental disorder and ER stress. In bipolar disorder patients, DNA microarray analysis of cell derived from twins discordant with respect to the disease revealed a down-regulated expression of genes related to ER stress responses such as x-box binding protein 1 (XBP1) and GRP78 [7]. In schizophrenia patients, a similar abnormality of these genes was found [8]. In addition, mood-stabilizing drugs such as valproate and lithium have been reported to increase the expression of GRP78, GRP94, and calreticulin [9]. Similarly, olanzapine, one of the second-generation "atypical" anti-psychotic drugs, appears to potentiates neuronal survival and neural stem cell differentiation by regulation of ER stress response proteins [10].

A recent study reported that significantly increased levels of GRP78, GRP94, and calreticulin were found in the temporal cortex of subjects with major depressive disorder who had died by suicide compared with control subjects who had died of other causes [11]. In addition, hippocampal atrophy [12] and reduction of glial density in the subgenual prefrontal cortex [13] were found in patients with major depression. Stress, a risk factor for depression, has been shown to induce atrophy of the apical dendrites of the hippocampal neurons [14], and to promote neuronal apoptosis in the cerebral cortex [15] in animal depression models. These findings suggest that a stressful situation, which may increase the risk for suicide, serves as an ER stressor. To clarify the relationship between exogenous stress and ER stress, in the present study, we investigated the expression of ER stress-related genes after restraint stress. We also focused on the elevation of corticosterone in the plasma and used a corticosterone-treated depression model to clarify the relationship between chronic corticosterone elevation and ER stress.

2. Materials and Methods

2.1. Animals

Male 9-week-old ddY mice and male 6-week-old ICR mice (Japan SLC, Hamamatsu, Japan) were used for all experiments. Mice were housed at 24 ± 2°C under a 12 hr light-dark cycle (lights on from 8:00 to 20:00) and had ad libitum access to food and water when not under restraint. Animals were acclimatized to laboratory conditions before the experiment. All procedures relating to animal care and treatment conformed to the animal care guidelines of the Animal Experiment Committee of Gifu Pharmaceutical University. All efforts were made to minimize both suffering and the number of animal used.

2.2. Restraint Stress

Male 9-week-old ddY mice (Japan SLC) weighing 30-40 g were used for real-time PCR studies. Mice were placed into 50-mL perforated plastic tubes, which prevented them from turning in any direction. Each mouse was maintained in the tube for 6 hr without any access to food or water.

2.3. Sampling

After this restraint stress, a blood sample was collected from the tail and the mouse was decapitated. The brain was quickly removed from the skull, briefly washed in ice-cold saline, and laid on a cooled (4°C) metal plate. The brain was rapidly dissected to separate the hippocampus, striatum, and cortex and stored at -80°C until use.

2.4. RNA Isolation

Total RNA was isolated from frozen brain using High Pure RNA Isolation Kit (Roche, Tokyo, Japan). RNA concentrations were determined spectrophotometrically at 260 nm. First-standed cDNA was synthesized in a 20-μl reaction volum using a random primer (Takara, Shiga, Japan) and Moloney murine leukemia virus reverse transcriptase (Invitrogen, Carlsbad, CA, USA).

2.5. Reai-Time PCR

Real-time PCR (TaqMan; Applied Biosystems, Foster City, CA, USA) was performed as described previously [16]. Single-standard cDNA was synthesized from total RNA using a high capacity cDNA archive kit (Applied Biosystems). Quantitative real-time PCR was performed using a sequence detection system (ABI PRISM 7900HT; Applied Biosystems) with a PCR master mix (TaqMan Universal PCR Master Mix; Applied Biosystems), according to the manufacturer's protocol. A gene expression product (Assays-on-Demand Gene Expression Product; Applied Biosystems) was used for measurements of mRNA expression by real-time PCR. The primers used for amplification were as follows: GRP78: 5'-GTTTG CTGAGGAAGACAAAAAGCTC-3' and 5'-CACTTCC ATAGAGTTTGCTGATAATTG-3'; CHOP: 5'-GGAG CTGGAAGCCTGGTATGAGG-3' and 5'-TCCCTGGT CAGGCGCTCGATTTCC-3'; GRP94: 5'-CTCACCATT TGGATCCTGTGTG-3' and 5'-CACATGACAAGATT TTACATCAAGA-3'; calreticulin: 5'-GCCAAGGACG AGCTGTAGAGAG-3' and 5'-GGTGAGGGCTGAAG GAGAATC-3'; ERdj4: 5'-TCTAGAATGGCTACTCCC CAGTCAATTTTC-3' and 5'-TCTAGACTACTGTCCT GAACAGTCAGTG-3'; EDEM: 5'-TGGGTTGGAAAG CAGAGTGGC-3' and 5'-TCCATTCCTACATGGAGG TAG-3'; p58IPK 5'-GAGGTTTGTGTTTGGGATGCAG-3' and 5'-GCTCTTCAGCTGACTCAATCAG-3'; ASNS: 5'-AGGTTGATGATGCAATGATGG-3' and 5'-TCCC CTATCTACCCACAGTCC-3'; β-actin: 5'-TCCTCCCT

GGAGAAGAGCTAC-3' and 5'-TCCTGCTTGCTGAT CCACAT-3' The thermal cycler conditions were as follows: 2 min at 50°C and then 10 min at 95°C, followed by two-step PCR for 50 cycles consisting of 95°C for 15s followed by 60°C for 1 min. For each PCR measurement, we checked the slope value, R^2 value, and linear range of a standard curve of serial dilutions. All reactions were performed in duplicate. The results were expressed relative to a β-actin internal control.

2.6. Measurement of Plasma Corticosterone

Plasma was obtained as described previously [17] and the concentration of corticosterone was determined *via* a corticosterone EIA kit (Assay Designs, Inc., Ann Arbor, MI, USA) according to the manufacturer's protocol.

2.7. Chronic Corticosterone Treatment

Male 6-week-old ICR mice (Japan SLC) weighing 20-25 g were used for chronic oral corticosterone exposure as described in a previous report [18]. Briefly, corticosterone (25 μg/mL free base; 4-pregnen-11β 21-DIOL-3 20-DIONE 21-hemisuccinate; Steraloids, Inc., RI, USA) was add to tap water and the pH was brought to 12-13 with 10 N NaOH (Kishidai Chemical, Osaka, Japan), followed by stirring at 4°C until dissolved (3 to 7 hr). Following dissolution, the pH was brought to 7.0-7.4 with 10 N HCl (Wako, Osaka, Japan). Group-housed ICR mice were presented with this corticosterone solution in place of normal drinking water for 14 days, resulting in a dose of approximately 8.7 mg/kg/day (p.o). Animals were weaned with 3 days of 12.5 μg/mL, and then 3 days with 6.25 μg/mL, to allow for gradual recovery of endogenous corticosterone secretion.

2.8. Western Blot Analysis

At 35 days, each mouse was decapitated and its brain was quickly removed from the skull, briefly washed in ice-cold saline, and laid on a cooled (4°C) metal plate. The brain was rapidly dissected to separate the hippocampus and stored at -80°C until use. Brain samples were homogenized in 10 mL/g tissue ice-cold lysis buffer [50 mM Tris-HCl (pH 8.0) containing 159 mM NaCl, 50 mM EDTA, 1% Triton X-100, and protease/phosphatase inhibitor mixture] using a homogenizer (Physcotron; Microtec Co. Ltd., Chiba, Japan). Lysates were centrifuged at 12,000×g for 15 min at 4°C. Supernatants were collected and boiled for 5 min in SDS sample buffer (Wako). Equal amounts of protein were subjected to 10% SDS-PAGE gradient gel and then transferred to poly (vinylidene difluoride) membranes (Immobilon-P; Millipore, MA, USA). After blocking with Block Ace (Snow Brand Milk Products Co. Ltd., Tokyo, Japan) for 30 min, the membranes were incubated with primary antibody. The primary antibodies used were as follows: mouse anti-BiP antibody (BD Bioscience, CA, USA) for GRP78, mouse anti-KDEL antibody (Stressgen Bioreagents Limited Partnership, B.C., Canada) for GRP94, and mouse anti-actin antibody (Sigma-Aldrich, St. Louis, MO, USA). Subsequently, the membrane was incubated with the secondary antibody [goat anti-mouse (Pierce Biotechnology, IL, USA)]. The immunoreactive bands were visualized using Super Signal West Femto Maximum Sensitivity Substrate (Pierce Biotechnology) and then measured using LAS-4000 mini (Fujifilm, Tokyo, Japan).

2.9. Statistical Analysis

Statistical comparisons were made by Student's *t*-test using Statview version 5.0 (SAS Institute Inc., NC, USA), with $p < 0.05$ being considered statistically significant.

3. Results and Discussion

Real-time PCR was carried out to investigate whether the expression of ER stress response-related genes in the brain was changed by 6-hr restraint stress. In this study, we investigated the expression of GRP94, carleticulin, ER degradation-enhancing α-mannosidase-like protein (EDEM), protein kinase inhibitor of 58 kDa ($p58^{IPK}$), asparagines synthetase (ASNS), GRP78, ER-localized DnaJ 4 (ERdj4), and C/EBP homologous protein (CHOP). The expression of GRP78, GRP94, and calreticulin mRNA was significantly increased in the hippocampus, striatum, and cortex (**Figure 1**). In addition, there was significantly increased expression of $p58^{IPK}$ mRNA in the cortex, but not in the hippocampus or striatum.

We next investigated whether restraint stress affected the plasma concentrations of corticosterone, as previously reported. Immediately following the 6-hr restraint stress, significantly higher plasma corticosterone concentrations were found in stressed mice compared to unstressed mice. Seven days after the restraint stress, the plasma corticosterone recovered to the normal control level (**Figure 2**).

To clarify the mechanism of ER stress-related mRNA elevation, we artificially elevated the plasma concentrations of corticosterone in mice for 2 weeks and then measured the levels of ER stress-related proteins. In the corticosterone-treated animal model, the expression of GRP78 and GRP94 in the hippocampus was significantly increased compared to control levels (**Figure 3**).

Restraint stress is used widely to induce stress responses in animals, and it is known that a number of stresses, including restraint stress, can cause depression in animals. In the present study, we found that several ER stress-related genes were increased in the mouse hippocampus, striatum, and cortex after restraint stress.

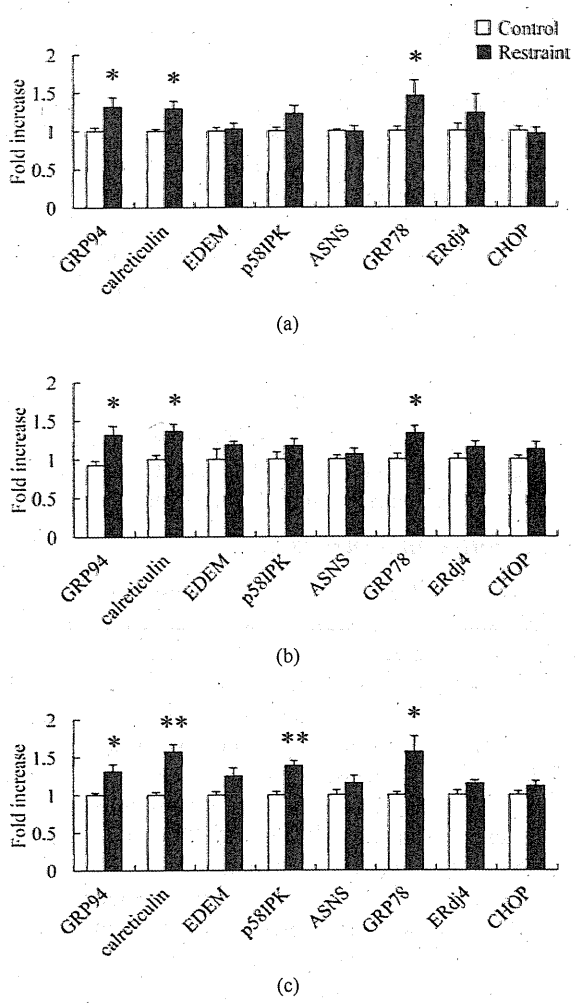

Figure 1. The expression mRNA of ER stress-related factors in the mouse brain after 6 hr restraint-stress. Mice were immobilized for 6 hr in a 50-mL perforated plastic tube. White and black bars represent the control group and the restraint group, respectively. Immediately after restraint, mice were killed and real-time PCR was performed on brain tissues from the (a) hippocampus, (b) striatum, and (c) cortex. Data represent means and S.E.M., n = 3 to 5. *p < 0.05, **p < 0.01 vs. control group. GRP94: the 94-kilodalton glucose regulated protein, EDEM: ER degradation-enhancing α-mannosidase-like protein, p58IPK: protein kinase inhibitor of 58 kilodalton, ASNS: asparagines synthetase, GRP78: the 78-kilodalton glucose regulated protein, ERdj4: ER-localized DnaJ 4, CHOP: C/EBP-homologous protein.

The significant increases in expression of GRP78, GRP94, and calreticulin agreed with the findings of a previous report of changes in the temporal cortex of subjects with major depression who died by suicide [11]. However, no study has yet specifically investigated expression changes of these genes in the hippocampus or the striatum in subjects with depression.

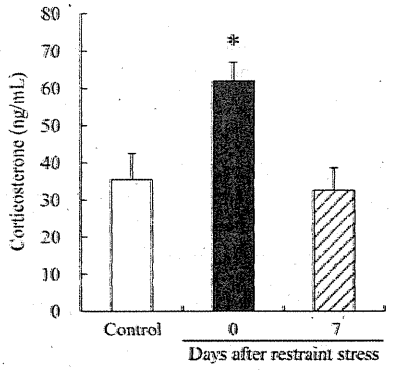

Figure 2. The effect of 6 hr restraint stress on the concentration of corticosterone in mouse plasma. Mice were immobilized for 6 hr. Immediately after restraint and 7 days later, blood samples were collected and concentration of plasma corticosterone was measured by ELISA. Restraint stress significantly increased the concentration of corticosterone in plasma. The corticosterone levels decreased to the normal control levels 7 days after restraint stress. Data represent means and S.E.M., n = 7. *p < 0.05 vs. control group.

GRP78, otherwise known as BiP, is one of the best-characterized ER chaperone proteins and is regarded as a classical marker of UPR activation. Overexpression of GRP78 has been reported to inhibit the upregulation of CHOP, which plays a key role in regulating cell growth and which has been implicated in apoptosis [19,20]. GRP94 and calreticulin are also ER chaperone proteins and show protective effects against ER stress [21]. The increase in these chaperones after restraint stress (**Figure 1**) may represent an attempt to oppose the toxic effect of prolonged stress and the high concentrations of glucocorticoid, such as corticosterone, on the brain. Dysregulation of the hypothalamic-pituitary-adrenal (HPA) axis, which controls glucocorticoid levels, has been reported in most depression patients and glucocorticoid level of depression patients was higher than those of normal ones [22-24]. In the mice in the present study, 6-hr restraint stress elevated the concentration of corticosterone in plasma, suggesting that restraint stress induced a response similar to depression.

Recently, corticosterone has been reported to exert immunostimulatory effects on macrophages *via* induction of ER stress [25]. Following corticosterone treatment, the glucocorticoid receptor (GR) binds onto B-cell lymphoma 2 (Bcl-2), a protein that affects cytochrome C and calcium release from mitochondria. Subsequently, this GR/Bcl-2 complex moves into mitochondria and regulates mitochondrial functions in an inverted "U"-shaped manner–i.e., a high dose treatment with corticosterone decreased levels of GRs and Bcl-2 in mitochondria and intracellular calcium was increased [26,27]. Substances

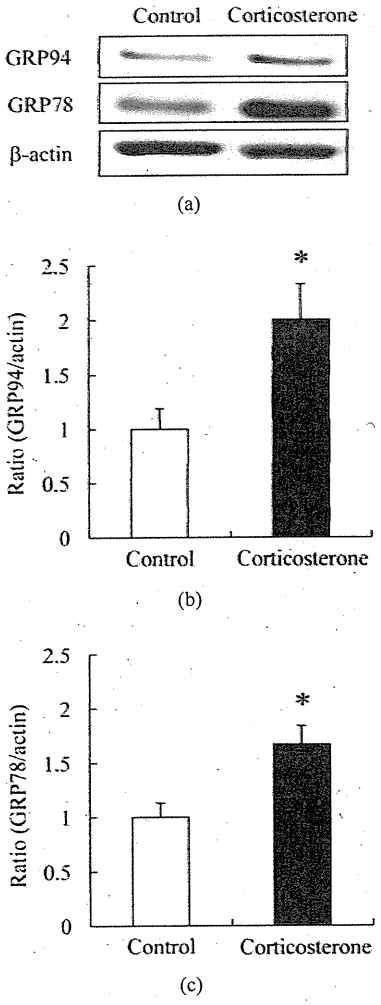

Figure 3. The expression of GRP78 and GRP94 in the hippocampus in a mouse model of chronic corticosterone induced depression. (a) Representative band images show immunoreactivities against GRP94, GRP78, and β-actin. (b) GRP78 expression was significantly increased by corticosterone exposure. (c) GRP94 expression was also increased by corticosterone exposure. Data represent means and S.E.M., n = 5 or 6. *p < 0.05 vs. control group.

that deplete the ER Ca^{2+} stores, such as thapsigargin, are widely used an ER stressors. Therefore, elevation of Ca^{2+} *via* GR may be sufficient for control of ER stress responses. In the present study, the restraint stress induced the expressions of only GRP78, GRP94, and calreticulin, but not other ER proteins. GRP78, GRP94, and calreticulin function as Ca^{2+} binding proteins [28]. Under the high concentration of corticosterone, the intracellular Ca^{2+} level might be higher, therefore, the expressions of GRP78, GRP94, and calreticulin might be increased.

Intracerebroventricular administration of thapsigargin has been reported to produce a depressant-like behavior [29]. A 14-days corticosterone treatment has also shown to induce depression symptoms in mice [18]. We used this animal model to investigate the effect of chronic elevation of corticosterone on ER stress responses in brain. As expected, significant increases in GRP78 and GRP94 proteins were observed in the hippocampus (**Figure 3**). The increase of GRP78 was consistent with the result of a previous report [30]. On the other hand, no change in these proteins was observed in the cortex (data not shown). Mineralocorticoid receptor (MR) and GR, which are the targets of corticosterone, are known to be well expressed in the hippocampus [31,32]. These reports, together with our findings, indicate that the hippocampus may be more sensitive to corticosterone exposure than are other brain regions. Many reports have referred to hippocampal atrophy in patients with depression [12,14]. In the cortex, it had been reported that chronic stress increased the caspase-3 positive neurons, in other words, exogenous stress was contributing to the cell apoptosis [15]. In our study, corticosterone exposure was performed for 2 weeks, but, in fact, long-term cortisol elevation has been observed in most depression patients. More extended corticosterone treatment may affect the expression of ER stress proteins in the cortex.

Recently, many experiments have focused on the relationship between depression and neurogenesis. Interestingly, ER stress also affects adult neurogenesis in the brain [33]. Brain-derived neurotrophic factor (BDNF), which promotes neurogenesis, is also known to inhibit neuronal cell death induced by ER stress [34]. These reports may also point to an involvement of ER stress in depression.

4. Conclusions

Restraint stress, which may contribute to depression in mice, may up-regulate the ER stress response *via* corticosterone elevation. This suggests the possibility of an ER stress involvement in the pathogenesis of stress-related depression disorders.

REFERENCES

[1] R. C. Kessler, P. Berglund, O. Demler, R. Jin, K. R. Me-rikangas and E. E. Walters, "Lifetime Prevalence and Age-of-onset Distributions of DSM-IV Disorders in the National Comorbidity Survey Replication," *Archives of general psychiatry*, Vol. 62, No. 6, 2005, pp. 593-602. doi:10.1001/archpsyc.62.6.593

[2] D. Ron and P. Walter, "Signal Integration in the Endoplasmic Reticulum Unfolded Protein Response," *Nature reviews*, Vol. 8, No. 7, 2007, pp. 519-529.

[3] V. I. Rasheva and P. M. Domingos, "Cellular Responses to Endoplasmic Reticulum Stress and Apoptosis," *Apoptosis*, Vol. 14, No. 8, 2009, pp. 996-1007.

 PP

doi:10.1007/s10495-009-0341-y

[4] S. Oyadomari and M. Mori, "Roles of CHOP/GADD153 in Endoplasmic Reticulum Stress," *Cell Death and Differentiation,* Vol. 11, No. 4, 2004, pp. 381-389. doi:10.1038/sj.cdd.4401373

[5] R. S. Saliba, P. M. Munro, P. J. Luthert and M. E. Chee-tham, "The Cellular Fate of Mutant Rhodopsin: Quality Control, Degradation and Aggresome Formation," *Journal of cell science*, Vol. 115, No. Pt 14, 2002, pp. 2907-2918.

[6] E. H. Koo, P. T. Lansbury, Jr. and J. W. Kelly, "Amyloid Diseases: Abnormal Protein Aggregation in Neurodegenera-tion," *Proceedings of the National Academy of Sciences of the United States of America*, Vol. 96, No. 18, 1999, pp. 9989-9990. doi:10.1073/pnas.96.18.9989

[7] C. Kakiuchi, K. Iwamoto, M. Ishiwata, M. Bundo, T. Kasahara, I. Kusumi, T. Tsujita, Y. Okazaki, S. Nanko, H. Kunugi, T. Sasaki and T. Kato, "Impaired Feedback Regulation of XBP1 as a Genetic Risk Factor for Bipolar disorder,"*Nature Genetics*, Vol. 35, No. 2, 2003, pp. 171-175. doi:10.1038/ng1235

[8] C. Kakiuchi, M. Ishiwata, T. Umekage, M. Tochigi, K. Kohda, T. Sasaki and T. Kato, "Association of the XBP1-116C/G Polymorphism with Schizophrenia in the Japanese Population," *Psychiatry and Clinical Neurosciences*, Vol. 58, No. 4, 2004, pp. 438-440. doi:10.1111/j.1440-1819.2004.01280.x

[9] L. Shao, X. Sun, L. Xu, L. T. Young and J. F. Wang, "Mood Stabilizing Drug Lithium Increases Expression of Endoplasmic Reticulum Stress Proteins in Primary Cultured Rat Cerebral Cortical Cells," *Life Sciences*, Vol. 78, No. 12, 2006, pp. 1317-1323. doi:10.1016/j.lfs.2005.07.007

[10] S. Kurosawa, E. Hashimoto, W. Ukai, S. Toki, S. Saito and T. Saito, "Olanzapine Potentiates Neuronal Survival and Neural Stem Cell Differentiation: Regulation of Endo-plasmic Reticulum Stress Response Proteins," *Journal of Neural Transmission*, Vol. 114, No. 9, 2007, pp. 1121-1128. doi:10.1007/s00702-007-0747-z

[11] C. Bown, J. F. Wang, G. MacQueen and L. T. Young, "Increased Temporal Cortex ER Stress Proteins in Depressed Subjects Who Died by Suicide," Neuropsychopharmacology, Vol. 22, No. 3, 2000, pp. 327-332. doi:10.1016/S0893-133X(99)00091-3

[12] Y. I. Sheline, P. W. Wang, M. H. Gado, J. G. Csernansky and M. W. Vannier, "Hippocampal Atrophy in Recurrent Major Depression," *Proceedings of the National Academy of Sciences of the United States of America*, Vol. 93, No. 9, 1996, pp. 3908-3913. doi:10.1073/pnas.93.9.3908

[13] D. Ongur, W. C. Drevets and J. L. Price, "Glial Reduction in the Subgenual Prefrontal Cortex in Mood Disorders," *Proceedings of the National Academy of Sciences of the United States of America*, Vol. 95, No. 22, 1998, pp. 13290-13295. doi:10.1073/pnas.95.22.13290

[14] Y. Watanabe, E. Gould and B. S. McEwen, "Stress Induces Atrophy of Apical Dendrites of Hippocampal CA3 Pyramidal Neurons," *Brain research*, Vol. 588, No. 2, 1992, pp. 341-345. doi:10.1016/0006-8993(92)91597-8

[15] A. Bachis, M. I. Cruz, R. L. Nosheny and I. Mocchetti, "Chronic Unpredictable Stress Promotes Neuronal Apoptosis in the Cerebral Cortex," *Neuroscience Letters*, Vol. 442, No. 2, 2008, pp. 104-108. doi:10.1016/j.neulet.2008.06.081

[16] D. Chen, E. Padiernos, F. Ding, I. S. Lossos and C. D. Lopez, "Apoptosis-stimulating Protein of P53-2 (ASPP2/53BP2L) is an E2F Target Gene," *Cell Death and Differentiation*, Vol. 12, No. 4, 2005, pp. 358-368. doi:10.1038/sj.cdd.4401536

[17] O. I. Abatan, K. B. Welch and J. A. Nemzek, "Evaluation of Saphenous Venipuncture and Modified Tail-clip Blood Collection in Mice," *Journal of the American Association for Laboratory Animal Science,*, Vol. 47, No. 3, 2008, pp. 8-15.

[18] S. L. Gourley and J. R. Taylor, "Recapitulation and Reversal of a Persistent Depression-like Syndrome in Rodents," *Current Protocols in Neuroscience* Chapter 9, 2009, Unit-9.32.

[19] X. Z. Wang, B. Lawson, J. W. Brewer, H. Zinszner, A. Sanjay, L. J. Mi, R. Boorstein, G. Kreibich, L. M. Hendershot and D. Ron, "Signals from the Stressed Endoplasmic Reticulum Induce C/EBP-homologous Protein (CHOP/GADD153)," *Molecular and Cellular Biology*, Vol. 16, No. 8, 1996, pp. 4273-4280.

[20] H. Zinszner, M. Kuroda, X. Wang, N. Batchvarova, R. T. Lightfoot, H. Remotti, J. L. Stevens and D. Ron, "CHOP is Implicated in Programmed Cell Death in Response to Impaired Function of the Endoplasmic Reticulum," *Genes & Development*, Vol. 12, No. 7, 1998, pp. 982-995. doi:10.1101/gad.12.7.982

[21] M. Cechowska-Pasko, "Endoplasmic Reticulum Chaperons," *Postepy Biochemii*, Vol. 55, No. 4, 2009, pp. 416-424.

[22] C. A. Sandman, J. L. Barron and L. Parker, "Disregulation of Hypothalamic-pituitary-adrenal Axis in the Mentally Retarded," *Pharmacology, Biochemistry, and Behavior*, Vol. 23, No. 1, 1985, pp. 21-26. doi:10.1016/0091-3057(85)90124-8

[23] A. Roy, "Hypothalamic-pituitary-adrenal Axis Function and Suicidal Behavior in Depression," Biological psychiatry, Vol. 32, No. 9, 1992, pp. 812-816. doi:10.1016/0006-3223(92)90084-D

[24] J. F. Lopez, D. M. Vazquez, D. T. Chalmers and S. J. Watson, "Regulation of 5-HT Receptors and the Hypothalamic-pituitary-adrenal Axis. Implications for the Neurobiology of Suicide," *Annals of the New York Academy of Sciences*, Vol. 836, No. 1, 1997, pp. 106-134.

[25] J. Y. Zhou, H. J. Zhong, C. Yang, J. Yan, H. Y. Wang and J. X. Jiang, "Corticosterone Exerts Immunostimulatory Effects on Macrophages via Endoplasmic Reticulum Stress," *The British Journal of Surgery*, Vol. 97, No. 2, 2010, pp. 281-293. doi:10.1002/bjs.6820

[26] J. Du, B. McEwen and H. K. Manji, "Glucocorticoid Receptors Modulate Mitochondrial Function: A Novel Mechanism for Neuroprotection," *Communicative & In-*

tegrative Biology, Vol. 2, No. 4, 2009, pp. 350-352.

[27] J. Du, Y. Wang, R. Hunter, Y. Wei, R. Blumenthal, C. Falke, R. Khairova, R. Zhou, P. Yuan, R. Machado-Vieira, B. S. McEwen and H. K. Manji, "Dynamic Regulation of Mitochondrial Function by Glucocorticoids," *Proceedings of the National Academy of Sciences of the United States of America*, Vol. 106, No. 9, 2009, pp. 3543-3548. doi:10.1073/pnas.0812671106

[28] H. Coe and M. Michalak, "Calcium Binding Chaperones of the Endoplasmic Reticulum," *General Physiology and Biophysics*, Vol. 28 Spec No Focus, 2009, pp. 96- 103.

[29] N. Galeotti, A. Bartolini and C. Ghelardini, "Blockade of Intracellular Calcium Release Induces an Antidepressant-like Effect in the Mouse Forced Swimming Test," *Neuropharmacology*, Vol. 50, No. 3, 2006, pp. 309-316. doi:10.1016/j.neuropharm.2005.09.005

[30] S. L. Gourley, F. J. Wu, D. D. Kiraly, J. E. Ploski, A. T. Kedves, R. S. Duman and J. R. Taylor, "Regionally Specific Regulation of ERK MAP Kinase in a Model of Antidepressant-sensitive Chronic Depression," Biological psychiatry, Vol. 63, No. 4, 2008, pp. 353-359. doi:10.1016/j.biopsych.2007.07.016

[31] T. Ito, N. Morita, M. Nishi and M. Kawata, "In Vitro and in Vivo Immunocytochemistry for the Distribution of Mineralocorticoid Receptor with the Use of Specific Antibody," *Neuroscience Research*, Vol. 37, No. 3, 2000, pp. 173-182. doi:10.1016/S0168-0102(00)00112-7

[32] F. Han, H. Ozawa, K. Matsuda, M. Nishi and M. Kawata, "Colocalization of Mineralocorticoid Receptor and Glucocorticoid Receptor in the Hippocampus and Hypothalamus," *Neuroscience Research*, Vol. 51, No. 4, 2005, pp. 371-381. doi:10.1016/j.neures.2004.12.013

[33] P. J. Lucassen, W. Scheper and E. J. Van Someren, "Adult Neurogenesis and the Unfolded Protein Response; New Cellular and Molecular Avenues in Sleep Research," *Sleep Medicine Reviews*, Vol. 13, No. 3, 2009, pp. 183-186. doi:10.1016/j.smrv.2008.12.004

[34] G. Chen, Z. Fan, X. Wang, C. Ma, K. A. Bower, X. Shi, Z. J. Ke and J. Luo, "Brain-derived Neurotrophic Factor Suppresses Tunicamycin-induced Upregulation of CHOP in Neurons," *Journal of Neuroscience Research*, Vol. 85, No. 8, 2007, pp. 1674-1684. doi:10.1002/jnr.21292

FEBS Letters 583 (2009) 394–400

FEBS Letters

journal homepage: www.FEBSLetters.org

Phosphorylated and ubiquitinated TDP-43 pathological inclusions in ALS and FTLD-U are recapitulated in SH-SY5Y cells

Takashi Nonaka [a,*], Tetsuaki Arai [b], Emanuele Buratti [c], Francisco E. Baralle [c], Haruhiko Akiyama [b], Masato Hasegawa [a,*]

[a] Department of Molecular Neurobiology, Tokyo Institute of Psychiatry, Tokyo Metropolitan Organization for Medical Research, 2-1-8 Kamikitazawa, Setagaya-ku 156-8585, Tokyo, Japan
[b] Department of Psychogeriatrics, Tokyo Institute of Psychiatry, Tokyo Metropolitan Organization for Medical Research, 2-1-8 Kamikitazawa, Setagaya-ku 156-8585, Tokyo, Japan
[c] International Centre for Genetic Engineering and Biotechnology, 34012 Trieste, Italy

ARTICLE INFO

Article history:
Received 31 October 2008
Revised 10 December 2008
Accepted 11 December 2008
Available online 25 December 2008

Edited by Barry Halliwell

Keywords:
TDP-43
FTLD-U
ALS
Phosphorylation
Ubiquitination

ABSTRACT

We report phosphorylated and ubiquitinated aggregates of TAR DNA binding protein of 43 kDa (TDP-43) in SH-SY5Y cells similar to those in brains of amyotrophic lateral sclerosis (ALS) and frontotemporal lobar degeneration with ubiquitinated inclusions (FTLD-U). Two candidate sequences for the nuclear localization signal were examined. Deletion of residues 78–84 resulted in cytoplasmic localization of TDP-43, whereas the mutant lacking residues 187–192 localized in nuclei, forming unique dot-like structures. Proteasome inhibition caused these to assemble into phosphorylated and ubiquitinated TDP-43 aggregates. The deletion mutants lacked the exon skipping activity of cystic fibrosis transmembrane conductance regulator (CFTR) exon 9. Our results suggest that intracellular localization of TDP-43 and proteasomal function may be involved in inclusion formation and neurodegeneration in TDP-43 proteinopathies.

1. Introduction

Frontotemporal lobar degeneration with ubiquitinated inclusions (FTLD-U) and amyotrophic lateral sclerosis (ALS) are well-known neurodegenerative disorders. FTLD is the second most common form of cortical dementia in the population below the age of 65 years [1]. ALS is the most common of the motor neuron diseases, being characterized by progressive weakness and muscular wasting, resulting in death within a few years. Ubiquitin (Ub)-positive inclusions were found as a pathological hallmark in brains of patients with FTLD-U and ALS, as well as in Alzheimer's disease (AD) and Parkinson's disease (PD). Recently, TAR DNA binding protein of 43 kDa (TDP-43) has been identified to be a major protein component of ubiquitin-positive inclusions in FTLD-U and ALS brains [2,3]. TDP-43 was first identified as a cellular factor that binds to the TAR DNA of HIV type 1 [4], and was also identified independently as part of a complex involved in inhibition of the splicing of the cystic fibrosis transmembrane conductance regulator (CFTR) gene [5]. TDP-43 aggregates in neuronal cytoplasm and nuclei in a variety of neurodegenerative disorders, which are now collectively referred to as TDP-43 proteinopathies. For understanding molecular pathogenesis and evidence-based therapies for TDP-43 proteinopathies, it is necessary to study the molecular mechanisms of aggregation of TDP-43.

To elucidate these issues, in this study, we have established the cellular models for intracellular aggregates of TDP-43 similar to those in brains of TDP-43 proteinopathies patients. Expression of deletion mutants of TDP-43 lacking two candidate sequences for the nuclear localization signal (NLS), residues 78–84 or 187–192, resulted in the formation of Ub- and phosphorylated TDP-43-positive cytoplasmic inclusions in the presence of a proteasome inhibitor. These results suggest that intracellular localization of TDP-43 and proteasomal function may be involved in the pathological process of TDP-43 proteinopathies.

Abbreviations: FTLD-U, frontotemporal lobar degeneration with ubiquitinated inclusions; ALS, amyotrophic lateral sclerosis; Ub, ubiquitin; TDP-43, TAR DNA binding protein of 43 kDa; CFTR, cystic fibrosis transmembrane conductance regulator; NLS, nuclear localization signal; TX, Triton X-100; Sar, Sarkosyl.

* Corresponding authors. Fax: +81 3 3329 8035 (T. Nonaka).
E-mail addresses: nonakat@prit.go.jp (T. Nonaka), masato@prit.go.jp (M. Hasegawa).

0014-5793/$34.00 © 2008 Federation of European Biochemical Societies. Published by Elsevier B.V. All rights reserved.
doi:10.1016/j.febslet.2008.12.031

2. Materials and methods

2.1. Construction of plasmids

The PCR product of the open-reading frame of human TDP-43 using pRc-CMV-TDP-43 as a template was subcloned into the mammalian expression vector pcDNA3 (Invitrogen) using restriction sites BamH I and Xba I, creating pcDNA3-TDP-43. To construct plasmids of the deletion mutants, we used a site-directed mutagenesis kit (Strategene). PCR was performed using the forward primer (5′-GTATGTTGTCAACTATATGGATGAGACAGATGC-3′) and the reverse primer (5′-GCATCTGTCTCATCCATATAGTTGACAACATAC-3′) for the deletion mutant of 78–84 residues (ΔNLS), and the forward primer (5′-GCAAAGCCAAGATGAGGTGTTTGTGGGGCGC-3′) and the reverse primer (5′-GCGCCCCACAAACACCTCATCTTGGCTTTGC-3′) for the deletion mutant of 187–192 residues (Δ187–192), with pcDNA3-TDP-43 as a template, respectively. For the construction of the double-deletion mutant ΔNLS&187–192, PCR was performed using the forward primer (5′-GCAAAGCCAAGATGAGGTGTTTGTGGGGCGC-3′) and the reverse primer (5′-GCGCCCCACAAACACCTCATCTTGGCTTTGC-3′) with pcDNA3-TDP-43ΔNLS as a template.

The reporter plasmid pSPL3-CFTR9 was constructed as follows. Healthy human genomic DNA (a gift from Dr. Makoto Arai, Tokyo Institute of Psychiatry, Japan) was subjected to PCR with the use of the forward primer (5′-CGGAATTCACTTGATAATGGGCAAATATC-3′) and the reverse primer (5′-CCCTCGAGCTCGCCATGTGCAAGATACAG-3′), containing EcoR I and Xho I sites, respectively. The genomic region containing 221 bp of intron 8, the entire exon 9 (183 bp), and 266 bp of intron 9 of the human CFTR gene was amplified and digested with the two restriction enzymes, followed by ligation into pSPL3 (Life Technologies), affording the plasmid pSPL3-CFTR9. All constructs were verified by DNA sequencing.

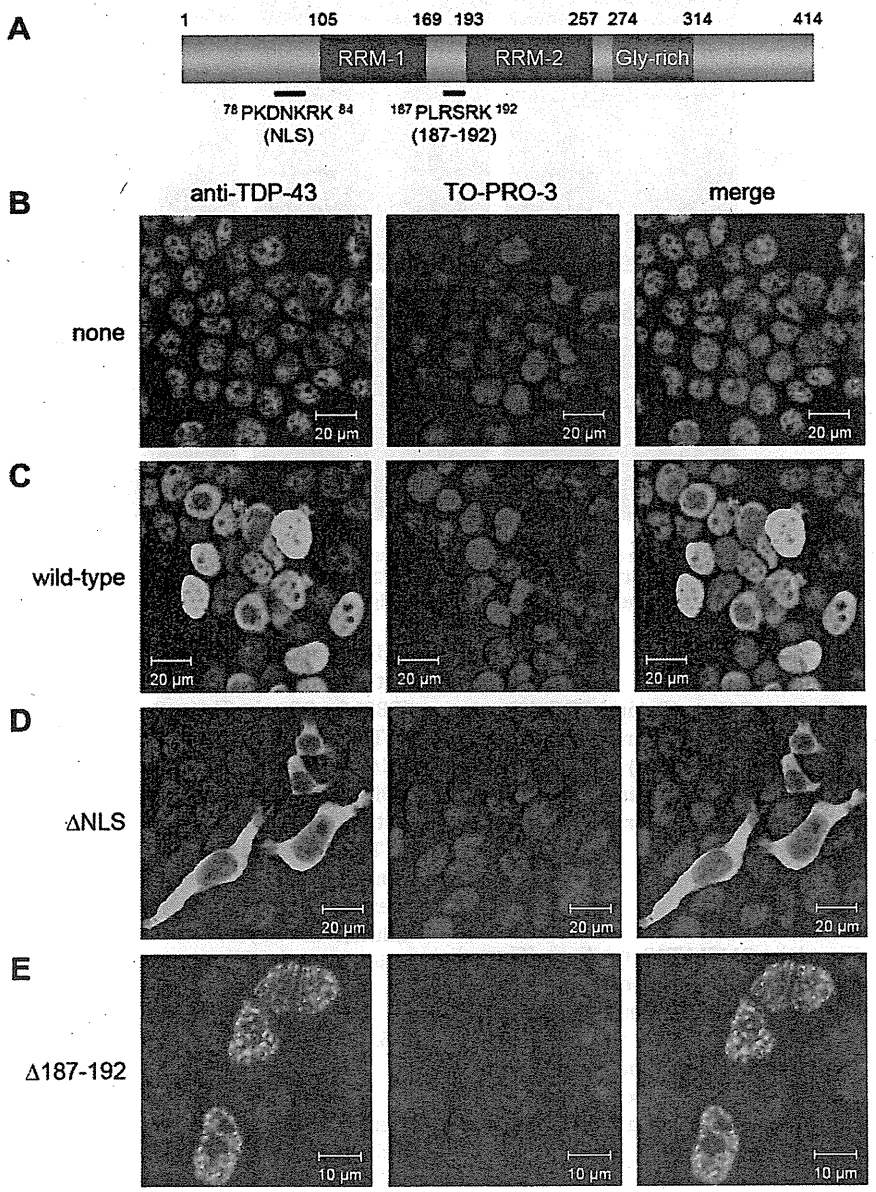

Fig. 1. Subcellular localization of wild–type and mutant TDP-43 in SH-SY5Y cells. (A) Schematic diagram of the structural domains of TDP-43. RNA recognition motifs (RRM-1 and -2: blue) and glycine-rich domain (Gly-rich: red) are shown. (B–E) Immunostaining of untransfected SH-SY5Y cells (B) and cells 72 h post transfection with wild-type TDP-43 (C), ΔNLS (Δ78–84) TDP-43 (D), and Δ187–192 TDP-43 (E) with anti-TDP-43 antibody (Left panel, green), nuclear staining by TO-PRO-3 (middle panel, blue) and the merged image (right panel) are shown.

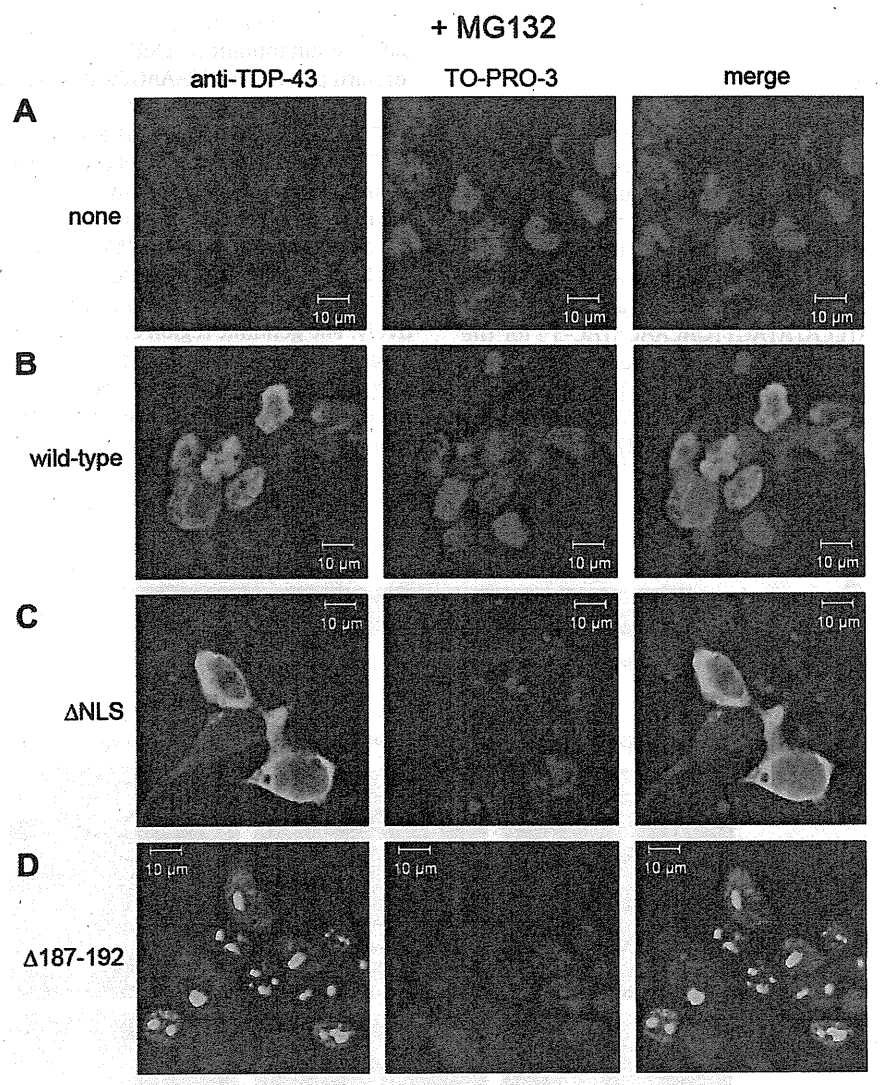

Fig. 2. Expression of mutant TDP-43 followed by proteasome inhibition with MG132 results in the formation of intranuclear inclusions. Immunostaining of untransfected cells (A) and cells 72 h post transfection with wild-type TDP-43 (B), ΔNLS (C), and Δ187–192 (D) followed by MG132 treatment (20 μM for 6 h) with anti-TDP-43 antibody (left panel, green), nuclear staining by TO-PRO-3 (middle panel, blue) and merged image (right panel).

2.2. Antibodies

A polyclonal TDP-43 antibody 10782-1-AP (anti-TDP-43) was purchased from ProteinTech Group Inc. A polyclonal antibody specific for phosphorylated TDP-43 (anti-pS409/410) was prepared as described [6]. Anti-ubiquitin monoclonal antibody (mAb), MAB1510, was purchased from Chemicon. Monoclonal anti-HA clone HA-7 were obtained from Sigma.

2.3. Cell culture and expression of plasmids

SH-SY5Y cells were cultured in DMEM/F12 medium (Sigma) supplemented with 10% (v/v) fetal calf serum, penicillin–streptomycin–glutamine (Gibco), and MEM non-essential amino acids solution (Gibco). Cells were then transfected with expression plasmids using FuGENE6 (Roche) according to the manufacturer's instructions. In the proteasome inhibition experiments, final 1 μM MG132 (Peptide institute) in DMSO was added to the culture medium, and incubated overnight.

2.4. Confocal immunofluorescence microscopy

SH-SY5Y cells were grown on a coverslip (15 × 15 mm) and transfected with expression vector (1 μg). After incubation for the indicated time, the transfected cells on the coverslips were fixed with 4% (w/v) paraformaldehyde in phosphate-buffered saline (PBS) for 30 min. The coverslips were then incubated with 0.2% (v/v) Triton X-100 (TX) in PBS for 10 min. After blocking for 30 min in 5% (w/v) BSA in PBS, cells were incubated with anti-phosphorylated TDP-43 antibody, pS409/410 (1:500 dilution), anti-TDP-43 (1:500), anti-Ub (1:500) or anti-HA (1:500) for 1 h at 37 °C, followed by FITC- or TRITC-labeled goat anti-rabbit or-mouse IgG (Sigma, 1:500 dilution) as a secondary antibody for 1 h at 37 °C. After washing, the cells were further incubated with TO-PRO-3 (Molecular Probes, 1:3000 dilution in PBS) for 1 h at 37 °C to stain nuclear DNA, and analyzed using a LSM5 Pascal confocal laser microscope (Carl Zeiss).

2.5. Sequential extraction of proteins and immunoblotting

SH-SY5Y cells were grown in 6-well plates and transfected transiently with expression plasmids (1 μg). After incubation for the indicated time, cells were harvested and lysed in TS buffer [50 mM Tris–HCl buffer, pH 7.5, 0.15 M NaCl, 5 mM ethylenediaminetetraacetic acid, 5 mM ethylene glycol bis(β-aminoethyl ether)-*N,N,N,N*-tetraacetic acid, and protease inhibitor cocktail (Roche)]. Lysates were centrifuged at 290,000×*g* for 20 min at 4 °C, and the supernatant was recovered as the TS-soluble fraction.